Insulin requires normal expression and signaling of insulin receptor A to reverse gestational diabetes–reduced adenosine transport in human umbilical vein endothelium

ARTICLE *in* THE FASEB JOURNAL · OCTOBER 2014

Impact Factor: 5.48 · DOI: 10.1096/fj.14-254219

12 AUTHORS, INCLUDING:

Marcelo Farias
Pontifical Catholic University of Chile
45 PUBLICATIONS **368** CITATIONS
SEE PROFILE

Pablo Arroyo Zúñiga
Pontifical Catholic University of Chile
13 PUBLICATIONS **45** CITATIONS
SEE PROFILE

Enrique Guzman-Gutierrez
San Sebastian University, Concepción, Chile
31 PUBLICATIONS **170** CITATIONS
SEE PROFILE

Andrea Leiva
Pontifical Catholic University of Chile
44 PUBLICATIONS **252** CITATIONS
SEE PROFILE

The FASEB Journal article fj.14-254219. Published online October 28, 2014.

Insulin requires normal expression and signaling of insulin receptor A to reverse gestational diabetes-reduced adenosine transport in human umbilical vein endothelium

Francisco Westermeier,*,† Carlos Salomón,*,‡ Marcelo Farías,* Pablo Arroyo,* Bárbara Fuenzalida,* Tamara Sáez,* Rocío Salsoso,* Carlos Sanhueza,* Enrique Guzmán-Gutiérrez,*,§ Fabián Pardo,* Andrea Leiva,* and Luis Sobrevia*,‡,¶,1

*Cellular and Molecular Physiology Laboratory (CMPL), Division of Obstetrics and Gynaecology, School of Medicine, Faculty of Medicine, Pontificia Universidad Católica de Chile, Santiago, Chile; †Advanced Center for Chronic Diseases (ACCDIS), Faculty of Chemical & Pharmaceutical Sciences, Universidad de Chile, Santiago, Chile; ‡University of Queensland Centre for Clinical Research (UQCCR), Faculty of Medicine and Biomedical Sciences, University of Queensland, Herston, Queensland, Australia; §Faculty of Health Sciences, Universidad San Sebastián, Concepción, Chile; and ¶Faculty of Pharmacy, Universidad de Sevilla, Seville, Spain.

ABSTRACT **Reduced adenosine uptake *via* human equilibrative nucleoside transporter 1 (hENT1) in human umbilical vein endothelial cells (HUVECs) from gestational diabetes mellitus (GDM) is reversed by insulin by restoring hENT1 expression. Insulin receptors A (IR-A) and B (IR-B) are expressed in HUVECs, and GDM results in higher *IR-A* mRNA expression *vs.* cells from normal pregnancies. We studied whether the reversal of GDM effects on transport by insulin depends on restoration of IR-A expression. We specifically measured hENT1 expression [mRNA, protein abundance, *SLC29A1* (for hENT1) promoter activity] and activity (adenosine transport kinetics) and the role of IR-A/IR-B expression and signaling [total and phosphorylated 42 and 44 kDa mitogen-activated protein kinases (p44/42^{mapk}) and Akt] in IR-A, IR-B, and IR-A/B knockdown HUVECs from normal (n = 33) or GDM (n = 33) pregnancies. GDM increases *IR-A/IR-B* mRNA expression (1.8-fold) and p44/42^{mapk}:Akt activity (2.7-fold) ratios. Insulin reversed GDM-reduced hENT1 expression and maximal transport capacity (V_{max}/K_m), and GDM-increased *IR-A/IR-B* mRNA expression and p44/42^{mapk}:Akt activity ratios to values in normal pregnancies. Insulin's effect was abolished in IR-A or IR-A/B knockdown cells. Thus, insulin requires normal IR-A expression and p44/42^{mapk}/Akt signaling to restore GDM-reduced hENT1 expression and activity in HUVECs. This could be a protective mechanism for the placental macrovascular endothelial dysfunction seen in GDM.—Westermeier, F., Salomón, C., Farías, M., Arroyo, P., Fuenzalida, B., Sáez, T., Salsoso, R., Sanhueza, C., Guzmán-Gutiérrez, E., Pardo, F., Leiva, A., Sobrevia, L. Insulin requires normal expression and signaling of insulin receptor A to reverse gestational diabetes-reduced adenosine transport in human umbilical vein endothelium. *FASEB J.* 29, 000–000 (2015). www.fasebj.org**

Key Words: endothelial dysfunction · human placenta · insulin signaling · nucleoside membrane transport

GDM IS CHARACTERIZED by glucose intolerance with an onset or first recognition during pregnancy (1) leading to adverse maternal and neonatal outcomes (2). In addition to defective placental insulin signaling (3–6), high plasma endogenous nucleoside adenosine has been reported in human umbilical veins (5–7) from GDM pregnancies. Even though increased endogenous nucleoside adenosine can result from increased transplacental transport of this nucleoside, it also may occur due to reduced umbilical vein endothelium adenosine uptake (5, 6). Adenosine dilates human umbilical vein rings *via* activation of adenosine receptors in HUVECs (5, 8). Because HUVECs lack

Abbreviations: $A_{2A}AR$, $A_{2A}AR$ adenosine receptor; β-IR, insulin receptor β-subunit; BMI, body mass index; GDM, gestational diabetes mellitus; hENT1, human equilibrative nucleoside transporter 1; HOMA-β, homeostasis model assessment for β cell function; HOMA-IR, homeostasis model assessment for insulin resistance; HOMA-IS, homeostasis model assessment for insulin sensitivity; hPMEC, human placental microvascular endothelial cells; HUVEC, human umbilical vein endothelial cells; IR-A, insulin receptor A; IR-B, insulin receptor B; MDT1, myotonic dystrophy type 1; NBTI, *S*-(4-nitrobenzyl)-6-thio-inosine; OGTT, oral glucose tolerance test; p42/44^{mapk}, 42 and 44 kDa mitogen-activated protein kinases; *SLC29A1*, solute carrier family 29 (equilibrative nucleoside transporter) member 1

[1] Correspondence: Cellular and Molecular Physiology Laboratory (CMPL), Division of Obstetrics and Gynaecology, School of Medicine, Faculty of Medicine, Pontificia Universidad Católica de Chile, P.O. Box 114-D, Santiago 8330024, Chile. E-mail: sobrevia@med.puc.cl

doi: 10.1096/fj.14-254219

This article includes supplemental data. Please visit *http://www.fasebj.org* to obtain this information.

extracellular adenosine deaminase activity to metabolize adenosine, maintenance of physiologic extracellular adenosine is achieved chiefly from endothelial uptake (9, 10). Thus, adenosine transport by HUVECs is crucial for regulating adenosine biologic activity (11). We previously reported that HUVECs from GDM pregnancies have lower expression and activity of hENT1 (5, 12), an Na^+-independent membrane transporter highly selective for nucleosides (13). GDM-associated reduction in hENT1 expression and activity leads to extracellular adenosine accumulation, resulting in A_{2A} adenosine receptor-dependent increases in eNOS and 42 and 44 kDa mitogen-activated protein kinases ($p42/44^{mapk}$) activity (14, 15).

Insulin restores GDM-associated reductions in hENT1 expression and activity in HUVECs (5); however, involvement of insulin receptors (IRs) and downstream associated cell signaling mechanisms remain unclear (16). Two IR isoforms generated by alternative splicing of exon 11 differing in the absence (IR-A) or presence (IR-B) of 12 amino acids at the α-subunit C-terminal has been identified (16–18). Insulin activates IR-A and IR-B in major insulin target tissues (16), including HUVECs (5) and human placenta microvascular endothelium (hPMEC) (6). Because IR-A or IR-B activation mediates either metabolic or mitogenic effects *via* protein kinase B/Akt (Akt) or $p44/42^{mapk}$ signaling pathways, respectively (6, 19), preferential expression of these IRs may change insulin sensitivity and cell responsiveness in HUVECs (9). Interestingly, whether IR-A and IR-B differential expression and activation change in HUVECs from GDM, and whether these potential changes are modulated by insulin in this cell type, are unknown (9). Thus, we hypothesized that IR-A and/or IR-B differential activation by insulin and their downstream signaling *via* $p42/44^{mapk}$ and Akt, respectively, result in reversal of GDM-associated reductions in hENT1-adenosine transport in HUVECs. Our data confirm this possibility, which may explain a crucial mechanism for maintaining physiologic fetal adenosine in GDM pregnancies.

MATERIALS AND METHODS

Study groups and human umbilical cords

Patients with basal glycemia <5 mM (<90 mg/dl, 8–9 h from last feeding) and >7.9 mM [>140 mg/dl 2 h after an oral glucose tolerance test (OGTT), 75 g glucose, measured between 24 and 28 wk of gestation) were diagnosed with gestational diabetes and subjected to dietary treatment with (1500 kcal/d and a maximum of 200 g per day carbohydrates; **Table 1**) (1). None of the patients diagnosed with GDM were previously diagnosed with GDM. Glycosylated hemoglobin A_{1c} was measured with HPLC, and glucose was measured with a hexokinase end-point method. Plasma insulin was measured by radioimmunoassay and homeostasis model assessment for insulin resistance (HOMA-IR) or sensitivity (HOMA-IS) and β-cell function (HOMA-β) (20, 21) were estimated as indicated in Table 1.

Umbilical cords were collected immediately after delivery from 33 full-term normal or 33 full-term GDM pregnancies from the public Universidad Católica Clinical Hospital in Santiago, Chile. The investigation conforms to the principles outlined in the Declaration of Helsinki. Ethics Committee approval from the Faculty of Medicine of the Pontificia Universidad Católica de Chile and patient written, informed consent were obtained 12–24 h before delivery. Sections of umbilical cords (100–120 mm length) were transferred into sterile 200 ml PBS solution [130 mM NaCl, 2.7 mM KCl, 0.8 mM Na_2HPO_4, 1.4 mM KH_2PO_4 (pH 7.4, 4°C)] to the laboratory and used for isolation of HUVECs from 2 to 6 h after delivery.

Cell culture

Confluent HUVEC primary cultures (37°C, 5% CO_2) were isolated by collagenase digestion (0.25 mg/ml Collagenase Type II from *Clostridium histolyticum*; Boehringer, Mannheim, Germany) as previously described (5) and were exposed to insulin (0.001–10 nM, 8 h) in medium 199 (M199; Gibco Life Technologies, Carlsbad, CA, USA) containing 5 mM D-glucose, 10% newborn calf serum (NBCS), 10% fetal calf serum (FCS), 3.2 mM L-glutamine, and 100 U/ml penicillin-streptomycin [primary culture medium (PCM)] (8), in the absence or presence of 10 μM PD-98059 (Calbiochem, La Jolla, CA, USA) or 30 nM wortmannin (Sigma-Aldrich, Atlanta, GA, USA). Experiments were done in confluent cells at passages 0 to 3 in culture. Meanwhile, freshly isolated uncultured cells were used for hENT1-adenosine transport assay and protein measurements. Cell viability was estimated with Trypan blue exclusion (8) values exceeding 97% for all culture passages. Cells were cultured in PCM containing 1% NBCS and 1% FCS for 24 h before performing the experiments (5, 8).

Adenosine transport

Total (overall) adenosine transport (*i.e.,* hENT1 + hENT2-mediated) was measured for increasing adenosine concentrations (0.15–500 μM) in the absence or presence of 1 μM *S*-(4-nitrobenzyl)-6-thio-inosine (NBTI; ENT1 inhibitor), 2 mM hypoxanthine (ENT2 substrate), or both as described (5, 6). The difference between total transport in the absence of NBTI or hypoxanthine and transport measured in the presence of 1 μM NBTI and 2 mM hypoxanthine was defined as ENT1-mediated transport, as previously described in HUVECs (5, 12). The remaining uptake activity detected in the presence of NBTI and 2 mM hypoxanthine (*i.e.,* NBTI/hypoxanthine-insensitive uptake) was ≤3% of total uptake of adenosine and unaltered over the entire range of adenosine concentrations used in this study for cells from both pregnancy types in the absence or presence of insulin.

Adenosine measurements with HPLC

Adenosine was measured with HPLC in whole brachial venous blood taken from 6 different women between 6 and 12 h before delivery and whole umbilical blood (vein + arteries) from the corresponding infants (*i.e.,* maternal-infant pairs) at birth, as described elsewhere (5, 6). Deproteinated samples were derivatized and stored until use for HPLC analysis (Isco HPLC system; Chemical Research Data Management System, Lincoln, NE, USA) (5, 6). Pearson correlation coefficient for a standard line of standard adenosine solution was >0.999 (range 2.996–439 nM), and the recovery of plasma adenosine was 83.1 ± 1.1% (n=6) (5, 6).

Reverse transcription and quantitative RT-PCR

Total RNA aliquots were reversed-transcribed into cDNA and subjected to real-time RT-PCR in an LightCycler rapid thermal

TABLE 1. *Clinical characteristics of women with normal or GDM pregnancies and newborns*

Variables	Normal (n = 33)	GDM (n = 33)
Maternal variables		
Age (y)	27 ± 4.6 (18–36)	30 ± 4.3 (18–38)
Height (cm)	159 ± 7.7 (147–177)	157 ± 6.1 (147–170)
Weight (kg)		
24–28 wg	65 ± 10 (54–77)	63 ± 10 (45–70)
38–40 wg	68 ± 2.0† (54–92)	64 ± 1.4† (45–86)
BMI (kg/m^2)		
24–28 wg	26 ± 1.9 (22–28)	25 ± 3.0 (20–28)
38–40 wg	26 ± 0.23 (22–29)	25 ± 0.37 (19–29)
Systolic blood pressure (mm Hg)		
24–28 wg	102 ± 5 (99–106)	104 ± 4 (99–109)
38–40 wg	107 ± 7 (103–110)	112 ± 6 (105–113)
Glycosylated hemoglobin A_{1c}		
24–28 wg (% of total) [mmol/mol]	4.2 ± 0.32 (3.2–5.0) [22 ± 2 (11–31)]	4.4 ± 0.15 (4.2–5.0) [25 ± 1 (22–31)]
38–40 wg (% of total) [mmol/mol]	4.0 ± 0.7 (3.2–5.1) [20 ± 4 (11–32)]	5.7 ± 0.29*,† (5.3–6.2) [39 ± 2 (34–44)]
Glycemia basal at delivery (mM)	4.5 ± 0.3 (3.9–5.0)	4.4 ± 0.3 (3.7–5.3)
OGTT (mM)		
Glycemia basal	4.4 ± 0.4 (3.7–5.1)	4.6 ± 0.4 (4.0–5.3)
Glycemia 2 h after glucose	5.4 ± 0.6 (3.6–6.2)	9.4 ± 1.8* (7.8–11.7)
Plasma insulin (μU/ml)	5.2 ± 0.3 (4.9–5.6)	7.9 ± 2.2* (5.9–11.6)
HOMA-IR	1.03 ± 0.08 (0.80–1.26)	1.59 ± 0.28* (1.02–2.73)
HOMA-IS (%)	97.5 ± 7.6 (79.3–125.2)	62.8 ± 11.0* (36.6–98.0)
HOMA-β (%)	110 ± 8.0 (70–450)	142 ± 25.5* (128–255)
Brachial blood adenosine (nM)[a]	189 ± 35 (110–276)	255 ± 56 (121–289)
Newborn variables		
Sex (female/male)	18/15	19/14
Gestational age (wk)	38.6 ± 1.0 (37–40)	38 ± 1.2 (37–40)
Birth weight (g)	3254 ± 0.4 (2600–4000)	3613 ± 0.44* (2920–4850)
Height (cm)	50 ± 1.6 (46–53)	49 ± 2.3 (43–55)
Ponderal index (g/cm^3 × 100)	2.6 ± 0.25 (2.1–3.5)	2.7 ± 0.27 (2.2–3.4)
Large for gestational age (%)	12	15
Umbilical vein D-glucose (mM)	3.7 ± 0.5 (3.1–4.4)	4.4 ± 0.5 (3.9–4.7)
Umbilical vein insulin (μU/ml)	6.0 ± 0.6 (5.1–7.3)	11.1 ± 0.5* (8.4–13.4)
HOMA-IR	0.98 ± 0.11 (0.70–1.42)	2.17 ± 0.17* (1.45–2.79)
HOMA-IS (%)	102 ± 11.9 (70.4–142.8)	46.1 ± 3.6* (35.8–68.9)
Umbilical cord blood adenosine (nM)[a]	229 ± 66 (119–301)	901 ± 127* (677–1102)

HOMA-IR was calculated from IR = Insulin/(22.5 × e (−ln (Glucose))) where insulin is in microunits per ml (μU/ml) and glucose is basal glycemia in millimoles (mM) as described elsewhere (20). Insulin sensitivity (IS) was derived from these values by $IS = (1/IR) \times 100$ (expressed in %). Additionally, HOMA-β (β−cell function, expressed in %) was estimated from HOMA $\beta = 20 \times$ (Insulin/(Glucose − 3.5)) as described elsewhere (20, 21). Values are mean ± SD (range). wg, weeks of gestation. OGTT was measured between 24 and 28 wg. [a]Values are for paired samples from 6 mothers and their children. *$P < 0.05$ *vs.* values in normal. †$P < 0.05$ *vs.* values at 24–28 wg in normal or GDM.

cycler (Roche Diagnostics, Lewes, United Kingdom) in the reaction buffer provided in the QuantiTectSYBR Green PCR Master Mix (Qiagen, Crawley, United Kingdom) using oligonucleotide primers for hENT1, IR-A, IR-B, and 28S (internal reference) as described elsewhere (5, 12). HotStart *Taq* DNA polymerase was activated (15 min, 95°C), followed by 40 cycles including denaturation (15 s) at 95°C, annealing (20 s) at 58°C (hENT1), 60°C (IR-A), 60°C (IR-B), 56°C (28S), and extension at 72°C (hENT1, 15 s; IR-A, 20 s; IR-B, 20 s; 28S, 10 s). *hENT1*, *IR-A*, or *IR-B* mRNA and *28S* rRNA reactions were run simultaneously in the same PCR reaction plate. Fluorescent product was detected after a 3 s step to 5°C below the product melting temperature (T_m). Product specificity was confirmed by agarose gel electrophoresis (1.8% v/v) and melting curve analysis. The product T_m values were 79.5°C for hENT1, 87.2°C for IR-A, 87.6°C for IR-B, and 82.4°C for 28S. The Ct value was defined as the PCR cycle number at which the fluorescent signal of the probes exceeded background and was used for calculating gene expression data with the $2^{-\Delta\Delta Ct}$ method (22).

IR β-subunit immunoprecipitation and Western blot

Total protein was obtained from cells washed (×2) with ice-cold PBS and harvested in 100 μl of lysis buffer [63.7 mM Tris/HCl (pH 6.8), 10% glycerol, 2% sodium dodecylsulfate, 1 mM sodium orthovanadate, 50 mg/ml leupeptin, 5% 2-mercaptoethanol] as described elsewhere (5, 6). Lysed proteins were sonicated (6 cycles, 5 s, 100 W, 4°C) and separated by centrifugation (12,000 *g*, 15 min, 4°C). Supernatant containing 500–1000 μg protein contained in 1000 μL lysis buffer were incubated (overnight, 4°C) with monoclonal mouse anti-IR β-subunit (β-IR) antibody (1: 5000; Sigma-Aldrich). Protein A/G plus IgG-agarose beads (KPL; Kirkegaard & Perry Laboratories, Incorporated, Baltimore, MD, USA) were added and the mixture was kept at 4°C for 1 h under gentle shaking. After washing (×6) with lysis buffer, the beads were pelleted (1000 *g*, 30 s), resuspended in 50 μL sample buffer [375 mM Tris-HCl (pH 6.8), 12% sodium dodecyl sulfate, 60% glycerol, 300 mM dithiothreitol, 0.06% bromophenol blue], and boiled for 5 min (23). The β-IR immunoprecipitate (100 μg)

diluted in sample buffer was separated by polyacrylamide gel (10%) electrophoresis (PAGE), transferred to Immobilon-P polyvinylidene difluoride membranes (BioRad Laboratories, Hertfordshire, United Kingdom), blocked (5% low-fat milk) in Tris-buffered saline Tween 20 solution (TBS-T) and incubated (1 h) in TBS-T/0.2% bovine serum albumin. The β-IR immunoprecipitates from normal or GDM pregnancies were then probed in parallel on the same membrane and with primary monoclonal rabbit anti-β-IR phosphorylated at tyrosine^{1361} (Tyr^{1361}; 1:1000 dilution, 1 h, 4°C; Cell Signaling, Danvers, MA, USA). Proteins were measured with enhanced chemiluminescence (5 min film exposure) and quantified with densitometry.

Western blot proteins (70 μg) separated by PAGE (10%) were probed with primary polyclonal goat anti-hENT1 (1:1000), anti-total and phosphorylated p42/44^{mapk} (1:1000) or Akt (1:1000; Cell Signaling), or anti-β-IR (1:5000) and monoclonal mouse anti-β-actin (1:5000, internal reference; Santa Cruz Biotechnology, Santa Cruz, CA, USA) antibodies, followed by 1 h incubation in TBS-T/0.2% bovine serum albumin (BSA) containing secondary horseradish peroxidase-conjugated goat anti-goat or anti-mouse antibodies (Santa Cruz Biotechnology), as described elsewhere (5, 12). Proteins from cells from normal or GDM pregnancies were assayed on the same immunoblot as described above.

Immunofluorescence microscopy

HUVECs were grown on microscope cover glasses (6×10^4 cells per slide; Sail Brand, Shanghai, China) in PCM to 90% confluency. Cells were cultured in 10% of PCM in the absence or presence of 1 nM insulin (8 h) and then fixed in 4% paraformaldehyde (5 min), rinsed (×3) with PBS, permeabilized with 0.2% Triton X-100 (10 min), and blocked (30 min) with 5% BSA and 0.02% Triton X-100. hENT1 was immunolocalized by incubating with primary monoclonal rabbit anti-hENT1 (1:30; Spring Bioscience, Pleasanton, CA, USA) overnight at 4°C in PBS containing 5% BSA (PBS/BSA). Incubated cells were then washed (×3) with PBS/BSA, followed by incubation (1 h, 22°C) with the secondary antibody Alexa Fluor 568 goat anti-rabbit IgG (H+L; $\lambda_{exc}/\lambda_{em}$: 578/603 nm; 1:500; Life Technologies) in PBS/BSA. Nuclei were counterstained with Hoescht 33342 (Life Technologies) and mounted with Fluoromount Aqueous Mounting Medium (Sigma-Aldrich). Images were obtained under an EVOS FL Imaging System (AMF 4300; Life Technologies).

hENT1 promoter cloning

Genomic DNA was isolated using the Wizard SV Genomic DNA Purification System (Promega, Madison, WI, USA). The sequences −3198 and −1670 bp from the ATG translation start codon of *SLC29A1* gene (GenBank: AF495730) were PCR-amplified using Elongase Enzyme System (Invitrogen, Carlsbad, CA, USA) and cloned into the pGL3-basic reporter system (12). The pGL3-hENT1 reporter constructs generated were pGL3-hENT1^{-3198} and pGL3-hENT1^{-1670}. For transient transfections, cells in suspension (3×10^6 cells/ml) were mixed with pGL3-hENT1 reporter constructs, pGL3-Basic (empty pGL3 vector), pGL3-Control [simian virus 40 promoter (SV40) pGL3 vector], or the internal transfection control vector pRL-TK expressing *Renilla* luciferase (Promega). Cells were electroporated (300 V, 700 μF, 5-10 ms; Gene Pulser II System, BioRad, Hercules, CA, USA) and cultured in M199 containing 2% fetal calf serum for 48 h before performing the experiments (12). *Firefly* and *Renilla* luciferase activity was measured using a Dual-Luciferase Reporter Assay System (Promega) in a Sirius luminometer (Berthold Detection System, Oak Ridge, TN, USA) (5, 12).

IR isoforms suppression

To suppress IR-A and IR-B expression, an adenoviral-based small interfering RNA (siRNA) delivering system (pSilencer adeno 1.0-CMV System Kit; Ambion, Austin, TX, USA) was used (6). Complementary oligonucleotides for IR-A and IR-B encoding for an siRNA hairpin targeting human IRs (GenBank: NM_001079817.1 for IR-A and NM_000208.2 for IR-B) were the following: IR-A sense 5′-GTTTTCGTCCCCAGGCCATCTTTCAAGAGAAGATGGCCTGGGGACGAAAAC-3′, IR-A antisense 5′-CAAAAGCAGGGGTCCGGTAGAAAGTTCTCTTCTACCGGACCCCTGCTTTTG-3′, IR-B sense 5′-GACCCTAGGCCATCTCGGAAATTCAAGAGATTTCCGAGATGGCCTAGGGTC-3′, IR-B antisense 5′-CTGGGATCCGGTAGAGCCTTTAAGTTCTCTAAAGGCTCTACCGGATCCCAG-3′. These oligonucleotides were designed following the General Design Guidelines provided by Ambion/Applied Biosystems (*http://www.lifetechnologies.com/cl/es/home/references/ambion-tech-support/rnai-sirna/general-articles/-sirna-design-guidelines.html*). The designed sequences were compared with potential target sites to the human genome database (using BLAST: *www.ncbi.nlm.nih.gov/BLAST*) discarding target sequences containing 16 or more contiguous base pairs of homology to other coding sequences and siRNAs with > 30% G/C content. The siRNA sequences providing at least 50% reduction in target mRNA levels were annealed and cloned into a pShuttle vector. The pShuttle-IR-A, pShuttle-IR-B siRNA, and the adenoviral LacZ backbone were linearized and transfected into HEK-293 cells to generate cells knockdown for IR-A (referred to as ^{KD}IR-A cells) or IR-B (referred to as ^{KD}IR-B cells) or both (referred to as ^{KD}IR-A/B cells). The negative control pShuttle vector (encoding a scramble siRNA sequence not found in human, mouse, or rat genome databases) was used to generate the negative control adenovirus. A positive siGAPDH provided by the kit was also used to generate an Ad-siGAPDH.

Recombinant adenoviral vectors were expanded by serial infection of HEK-293 cells, harvested by a three freeze-thaw procedure, and used to infect HUVECs (6). Adenoviral particles were purified and quantified before experiments using a commercial kit (ViralBind Adenovirus Purification Kit, Cell Biolabs, San Diego, CA, USA). Cells at 50–60% confluence were seeded 24 h before adenoviral infection. Viral stocks were diluted to reach the desired multiplicity of infection (MOI) in serum-free medium and added to the cell monolayer (**Supplemental Fig. 1**). Non-infected (hereafter referred to as "nontransduced") and infected (hereafter referred to as "transduced") cells were incubated with serum-free medium for 8 h. Then, the infective medium was changed to complete culture medium, and cells were incubated for a further 48 h under standard culture conditions. Isolation of total RNA and protein and functional assays were then performed as described previously.

Statistical analyses

Values are means ± SEM or SD, with $n = 33$ different cell cultures (2–4 replicates) from normal or GDM pregnancies. Because the HUVECs yield from 1 single placenta were not enough to proceed with all experimental strategies included in this study, the reported n value is variable and corresponds to paired cell cultures from normal and GDM pregnancies. Data reported here describe a normal standard distribution. Comparisons between 2 or more groups were performed with the Student's unpaired t test or ANOVA, respectively, followed by *post hoc* analyses performed using a multiple-comparison Bonferroni correction test. Statistical software GraphPad Instat 3.0b and Graphpad Prism 6.0d (GraphPad Software Incorporated, San Diego, CA, USA) were used for data analysis. $P < 0.05$ was considered statistically significant.

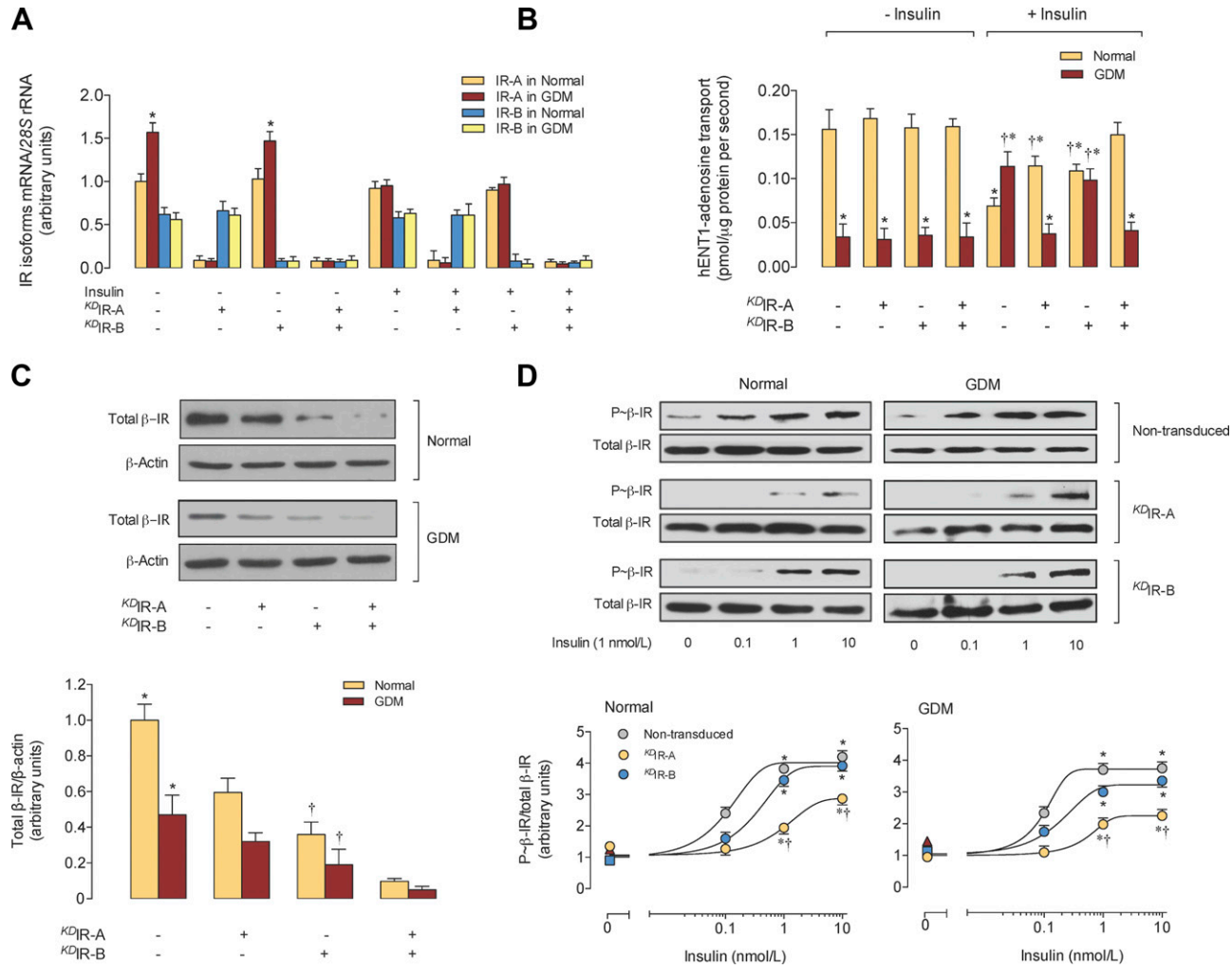

Figure 1. Insulin requires IR-A expression to restore GDM-reduced hENT1-adenosine transport. *A*) *IR-A* or *-B* mRNA level compared with *28S* rRNA (internal reference) in HUVEC from normal or GDM pregnancies, in the absence (–Insulin) or presence (+Insulin) of insulin (1 nM, 8 h) in nontransduced (–) or transduced (+) cells with adenovirus containing siRNA against IR-A (^{KD}IR-A) or -B (^{KD}IR-B). Values are normalized to 1 in *IR-A* mRNA in cells from normal pregnancies. *B*) Adenosine transport *via* hENT1 as in *A*. *C*) Western blot for total β-IR (nonphosphorylated + phosphorylated forms; total β-IR) and β-actin (internal reference) protein abundance in the absence of insulin in cells as in *A*. Lower panel: Total β-IR:β-actin ratio densitometries normalized to 1 in nontransduced cells from normal. *D*) Western blot for total β-IR or phosphorylated β-IR (P-β-IR) in response to insulin (8 h) in nontransduced, ^{KD}IR-A, or ^{KD}IR-B cells. Lower panels: P-β-IR:total β-IR protein abundance ratio densitometries normalized to 1 in nontransduced cells from normal. *A*) $^{*}P < 0.03$ *vs.* all other values. *B*) $^{*}P < 0.05$ *vs.* nontransduced cells from normal in –Insulin. $^{\dagger}P < 0.04$ *vs.* corresponding values in –Insulin. *C*) $^{*}P < 0.04$ *vs.* all other corresponding values. $^{\dagger}P < 0.05$ *vs.* corresponding values in ^{KD}IR-A or ^{KD}IR-A/B cells. *D*) $^{*}P < 0.05$ *vs.* corresponding values in 0 or 0.1 nM insulin. $^{\dagger}P < 0.05$ *vs.* corresponding values in nontransduced or ^{KD}IR-B cells. Values are mean ± SEM (n = 18–21).

RESULTS

Patients and newborns

Normal or GDM pregnancies were singleton, and pregnant women were normotensive and nonsmoking, did not consume alcohol or drugs, and were without intrauterine infection or any other medical or obstetric complication (Table 1). Newborns from GDM pregnancies were large for gestational age and heavier at birth, with higher umbilical vein insulin and HOMA-IR but lower HOMA-IS compared with newborns from normal pregnancies. Maternal blood adenosine was similar between normal and GDM pregnancies at birth; however, adenosine in whole umbilical blood was higher (3.9 ± 0.5-fold) in GDM compared with normal pregnancies (Table 1).

IR isoforms, adenosine transport, and β-IR expression

IR-A mRNA was higher than *IR-B* mRNA level in HUVECs from normal or GDM pregnancies (**Fig. 1*A***). Insulin reversed the increase of *IR-A* mRNA level in cells from GDM to values similar to normal pregnancies. This effect was abolished either in ^{KD}IR-A, ^{KD}IR-B, or ^{KD}IR-A/B cells from normal or GDM pregnancies. IRs mRNA level was largely reduced in ^{KD}IR-A and ^{KD}IR-B cells (Supplemental Fig. 1).

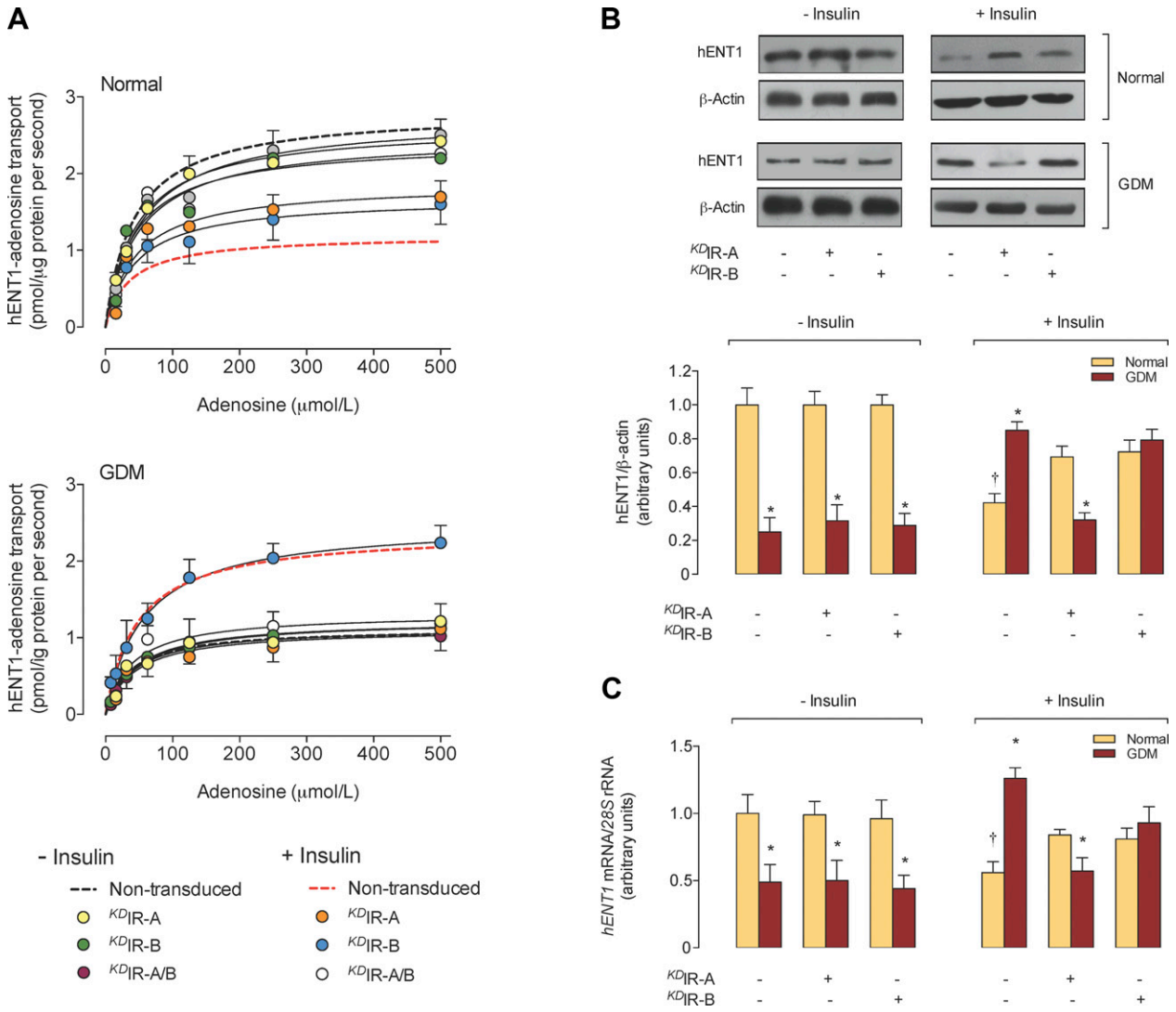

Figure 2. Insulin restores transport activity and expression of hENT1 *via* IR-A in GDM. *A*) Kinetics of hENT1-mediated adenosine transport (4 μCi/ml [^{3}H]adenosine, 20 s, 22°C) in nontransduced or transduced cells with adenovirus containing siRNA against IR-A (^{KD}IR-A), -B (^{KD}IR-B), or both (^{KD}IR-A/B), from normal or GDM pregnancies. Assays were done in the absence (–Insulin) or presence (+Insulin) of insulin (1 nM, 8 h). *B*) Western blot for hENT1 protein abundance in nontransduced (–) or transduced (+) cells as in *A*. Lower panel: hENT1:β-actin ratio densitometries normalized to 1 in –Insulin in Normal pregnancies. β-Actin is the internal reference. *C*) Expression of *hENT1* mRNA level compared with *28S* rRNA (internal reference) in cells as in *A*. Values are normalized to 1 in *hENT1* mRNA in nontransduced cells from normal. *B*) $^*P < 0.01$ *vs.* corresponding values in Normal pregnancies. $^\dagger P < 0.04$ *vs.* all other values in normal pregnancies and nontransduced or ^{KD}IR-B cells from GDM in +Insulin. *C*) $^*P < 0.04$ *vs.* corresponding values in normal pregnancies. $^\dagger P < 0.05$ *vs.* all other values in normal pregnancies and nontransduced or ^{KD}IR-B cells from GDM in +Insulin. Values are mean ± SEM (n = 17–19).

In addition, ^{KD}IR-A or ^{KD}IR-B cells had lower *IR-A* or *IR-B* mRNA levels and *IR-B* or *IR-A* mRNA level was not changed, respectively. Similar results occurred in cells after culture for different periods of time (passages 0, 1, 2, or 3) (**Supplemental Fig. 2**).

hENT1-adenosine transport was lower in GDM cells compared with normal pregnancies, and insulin reduced hENT1-adenosine transport in normal pregnancies but restored the GDM-associated transport reduction to values in normal pregnancies (Fig. 1B), confirming previous results in HUVECs (5, 12). Freshly isolated, uncultured cells and cells passaged 0, 1, or 2 times had a similar reduction in hENT1-adenosine transport (**Supplemental Fig. 3**) compared with passage 3 cells (Fig. 1*B*). In normal pregnancies, insulin reduction of hENT1-adenosine uptake was partial in ^{KD}IR-A or ^{KD}IR-B cells but blocked in ^{KD}IR-A/B cells. However, in GDM the effect of insulin was blocked in ^{KD}IR-A or ^{KD}IR-A/B cells but not in ^{KD}IR-B cells. In the absence of insulin, hENT1-adenosine uptake was unaltered in ^{KD}IR-A, ^{KD}IR-B, or ^{KD}IR-A/B cells from normal or GDM pregnancies.

Total β-IR subunit protein in cells expressing IR-A and IR-B was lower for GDM compared with normal pregnancies (Fig. 1*C*). A larger reduction was seen for total β-IR subunit protein in ^{KD}IR-B compared with ^{KD}IR-A cells, and it was almost abolished in ^{KD}IR-A/B cells both from normal or GDM pregnancies. Insulin increased Tyr^{1361} phosphorylation of the β-IR subunit (P-β-IR) increasing the P-β-IR:total β-IR ratio and reaching similar maximal values with comparable ($P < 0.05$) half-maximal stimulatory effects

TABLE 2. *Effect of GDM and IRs isoforms involvement on hENT1-mediated adenosine transport*

	Normal			GDM		
	V_{max} (pmol/μg protein per second)	K_m (μM)	V_{max}/K_m (pmol/μg protein per second)/(μM)	V_{max} (pmol/μg protein per second)	K_m (μM)	V_{max}/K_m (pmol/μg protein per second)/(μM)
Nontransduced cells						
Control	2.82 ± 0.17	43 ± 9	0.066 ± 0.006	1.12 ± 0.04*	36 ± 4	0.031 ± 0.003*
PD-98059	2.79 ± 0.10	43 ± 5	0.065 ± 0.006	2.94 ± 0.12†	53 ± 7	0.055 ± 0.006†
Wortmannin	2.93 ± 0.18	37 ± 7	0.079 ± 0.006	0.96 ± 0.09	33 ± 7	0.029 ± 0.003
PD-98059 + wortmannin	2.85 ± 0.12	49 ± 7	0.058 ± 0.004	2.91 ± 0.08†	53 ± 5	0.055 ± 0.006†
Insulin	1.19 ± 0.05*	35 ± 5	0.034 ± 0.002*	2.39 ± 0.21†	47 ± 9	0.051 ± 0.006†
Insulin + PD-98059	2.99 ± 0.20	44 ± 9	0.068 ± 0.005	2.63 ± 0.22†	50 ± 10	0.053 ± 0.007†
Insulin + wortmannin	2.79 ± 0.24	36 ± 9	0.078 ± 0.004	2.78 ± 0.15†	53 ± 9	0.052 ± 0.004†
Insulin + PD-98059 + wortmannin	3.14 ± 0.14	43 ± 7	0.073 ± 0.009	2.73 ± 0.13†	49 ± 8	0.056 ± 0.005†
^{KD}IR-A cells						
Control	2.62 ± 0.08	46 ± 5	0.057 ± 0.005	1.23 ± 0.09*	44 ± 9	0.028 ± 0.002*
PD-98059	2.41 ± 0.28	38 ± 19	0.063 ± 0.009	2.65 ± 0.27†	45 ± 18	0.058 ± 0.008†
Wortmannin	2.63 ± 0.13	37 ± 8	0.071 ± 0.009	1.33 ± 0.13	44 ± 17	0.030 ± 0.004
Insulin	1.87 ± 0.18*	46 ± 9	0.041 ± 0.004*	1.11 ± 0.09*	43 ± 8	0.026 ± 0.003*
Insulin + PD-98059	2.33 ± 0.16	45 ± 12	0.052 ± 0.008	2.71 ± 0.22†	42 ± 14	0.065 ± 0.006†
Insulin + wortmannin	2.74 ± 0.24	40 ± 15	0.069 ± 0.005	1.35 ± 0.16	35 ± 18	0.039 ± 0.005
^{KD}IR-B cells						
Control	2.53 ± 0.23	48 ± 9	0.053 ± 0.004	1.23 ± 0.04*	49 ± 5	0.025 ± 0.003*
PD-98059	2.49 ± 0.28	37 ± 7	0.067 ± 0.007	2.42 ± 0.25†	38 ± 17	0.064 ± 0.007†
Wortmannin	2.55 ± 0.23	40 ± 15	0.064 ± 0.007	1.21 ± 0.13	35 ± 16	0.035 ± 0.006
Insulin	1.30 ± 0.13*	47 ± 8	0.028 ± 0.003*	2.50 ± 0.07†	32 ± 5	0.078 ± 0.007†
Insulin + PD-98059	2.76 ± 0.21	50 ± 15	0.055 ± 0.009	2.47 ± 0.23†	38 ± 15	0.065 ± 0.008†
Insulin + wortmannin	2.61 ± 0.19	36 ± 11	0.073 ± 0.009	2.75 ± 0.23†	43 ± 15	0.064 ± 0.007†
^{KD}IR-A/B cells						
Control	2.63 ± 0.14	48 ± 8	0.055 ± 0.004	1.14 ± 0.03‡	40 ± 4	0.029 ± 0.003‡
Insulin	2.49 ± 0.21	47 ± 7	0.053 ± 0.005	1.32 ± 0.09‡	39 ± 9	0.034 ± 0.003‡

hENT1-mediated adenosine transport in HUVEC from normal or GDM pregnancies was measured as described under Materials and Methods. Cells were not transduced or transduced with siRNA against IR-A (^{KD}IR-A), IR-B (^{KD}IR-B), or both isoforms (^{KD}IR-A/B) of IRs. Transport was measured in the absence (control) or presence (8 h) of 1 nM insulin and/or 10 μM PD-98059 or 30 nM wortmannin. V_{max} and K_m of saturable transport were determined. V_{max}/K_m is maximal transport capacity. Values are mean ± SEM ($n = 19$). *$P < 0.05$ *vs.* corresponding values for control in normal. $^{\dagger}P < 0.05$ *vs.* corresponding values for control in GDM. $^{\ddagger}P < 0.05$ versus corresponding values in normal.

(SC_{50}) in nontransduced cells from normal ($SC_{50} = 0.12 \pm 0.03$ nM) and GDM ($SC_{50} = 0.11 \pm 0.02$ nM) pregnancies (Fig. 1*D*). The maximal effect of insulin on P-β-IR:total β-IR ratio was lower ($P < 0.04$) in ^{KD}IR-A compared with nontransduced cells in normal and GDM pregnancies. However, SC_{50} for insulin's effect in ^{KD}IR-A cells from normal pregnancies was higher ($SC_{50} = 0.99 \pm 0.02$ nM, $P < 0.05$) compared with cells from GDM pregnancies ($SC_{50} = 0.55 \pm 0.02$ nM). Maximal increases in the P-β-IR: total β-IR ratio and SC_{50} values were unaltered ($P > 0.05$) in ^{KD}IR-B cells from normal ($SC_{50} = 0.35 \pm 0.04$ nM) and GDM ($SC_{50} = 0.21 \pm 0.02$ nM) pregnancies and were similar to values in nontransduced cells from normal or GDM pregnancies.

Kinetics of hENT1-adenosine transport and hENT1 expression

hENT1-adenosine transport was saturable in cells from normal and GDM pregnancies (Fig. 2*A*). A lower V_{max} and V_{max}/K_m for hENT1-adenosine, transport was seen in nontransduced cells from GDM compared with normal pregnancies, an effect blocked by insulin (**Table 2**). Similar results were found for hENT1-adenosine transport in ^{KD}IR-A or ^{KD}IR-B cells in normal and GDM pregnancies in the absence of insulin. However, insulin re-establishment of the V_{max}/K_m for hENT1-adenosine transport in nontransduced cells was blocked in ^{KD}IR-A, but not in ^{KD}IR-B cells from GDM pregnancies. Additional assays show that GDM's effect on hENT1-adenosine transport persisted in ^{KD}IR-A/B cells (Table 2).

hENT1 protein was lower in cells from GDM compared with normal pregnancies and in ^{KD}IR-A or ^{KD}IR-B cells in the absence of insulin (Fig. 2*B*). Insulin restored hENT1 protein in cells from GDM, an effect abolished in ^{KD}IR-A, but not in ^{KD}IR-B cells. The reduction in hENT1 protein caused by insulin was partially reversed in ^{KD}IR-A or ^{KD}IR-B cells from normal pregnancies. *hENT1* mRNA level had similar patterns with respect to protein in normal and GDM pregnancies in the absence of insulin (Fig. 2*C*). However, insulin-reduced *hENT1* mRNA level in cells from normal pregnancies and restoration of *hENT1* mRNA level by insulin in GDM pregnancies was lower in ^{KD}IR-A or ^{KD}IR-B cells. In assays using freshly isolated cells from normal and GDM pregnancies exposed to insulin, hENT1 protein (**Supplemental Fig. 4**) was not significantly different from data obtained in cells at passage 3.

Immunocytochemical assays show that hENT1 protein was located mainly at the cell border in cells from normal pregnancies but predominantly at intracellular structures

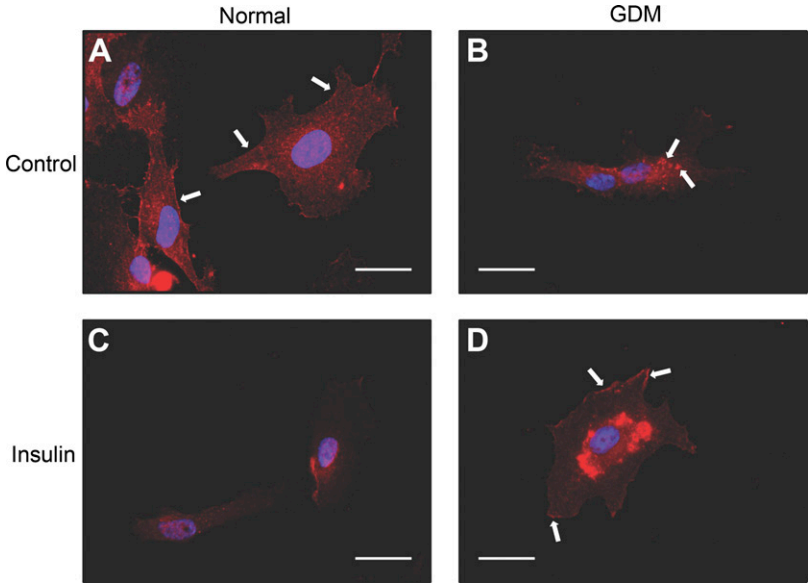

Figure 3. Insulin modulates in a differential manner the hENT1 cell localization in endothelial cells from normal or GDM pregnancies. Immunocytochemistry of hENT1 (red fluorescence) in HUVEC from normal or GDM pregnancies. Cells were incubated in primary culture medium without (control) (*A*, *B*) or with 1 nM insulin (8 h) (*C*, *D*). Nuclei (blue fluorescence) were counterstained with Hoescht 33342 and mounted with Fluoromount Aqueous Mounting Medium (see Materials and Methods). Arrows show hENT1 fluorescence at the plasma membrane (*A*, *D*) and intracellular space (*B*). Images are representative of 11 different experiments from 11 pregnant women coursing with normal pregnancies or equal number of women coursing with GDM pregnancies. Bars indicate 25 μm at $\times$60 microscopy magnification.

in cells from GDM pregnancies (**Fig. 3**). Incubation of cells with insulin reduced the fluorescent signal at the cell border for hENT1 in normal pregnancies; however, hENT1 fluorescence was higher at the cell border in GDM pregnancies.

SLC29A1 promoter transcriptional activity

SLC29A1 promoter luciferase activity in the absence of insulin was similar in cells from normal pregnancies transfected with pGL3-hENT1^{-3198} or pGL3-hENT1^{-1670} constructs (**Fig. 4*A***). However, pGL3-hENT1^{-3198} promoter luciferase activity in GDM was lower compared with pGL3-hENT1^{-1670} construct promoter activity in cells from GDM and from normal pregnancies in the absence of insulin. Cells from normal pregnancies had less pGL3-hENT1^{-3198} reporter activity in response to insulin; however, insulin restored reporter activity in GDM to values in cells from normal pregnancies without insulin. Insulin's effect was partially reduced in ^{KD}IR-A or ^{KD}IR-B cells but blocked in ^{KD}IR-A/B cells in normal or GDM pregnancies. The fraction of insulin's effect on pGL3-hENT1^{-3198} reporter activity requiring IR-A or IR-A/IR-B expression was higher in GDM compared with normal pregnancies (Fig. 4*B*). However, the IR-B expression requirement for insulin's effect on this construct was similar in normal and GDM pregnancies. In addition, the fraction of insulin's effect requiring expression of IR-A, IR-B, or IR-A/IR-B on pGL3-hENT1^{-1670} reporter activity was unaltered by GDM (Fig. 4*C*).

Involvement of p42/44^{mapk} and Akt on hENT1-adenosine transport

GDM-associated reduction in hENT1-adenosine transport was blocked by PD-98059 (MAPK kinase inhibitor) or PD-98059 + wortmannin (PI3K inhibitor) but not by wortmannin in nontransduced cells in the absence of insulin (Table 2). However, neither PD-98059 nor wortmannin altered transport in nontransduced cells from normal pregnancies in the absence of insulin. Insulin-restored hENT1-adenosine transport was unaltered by PD-98059 and/or wortmannin in nontransduced cells from GDM. However, these inhibitors blocked insulin inhibition of hENT1-adenosine transport in cells from normal pregnancies. These events coincided with increased p42/44^{mapk} phosphorylation in nontransduced cells in the absence of insulin from GDM compared with normal pregnancies (**Fig. 5*A***). Insulin increased p42/44^{mapk} phosphorylation in cells from normal pregnancies but reduced p42/44^{mapk} phosphorylation in cells from GDM to values similar to those in normal pregnancies. Incubation of cells with PD-98059 abolished p42/44^{mapk} phosphorylation in the absence or presence of insulin. In contrast, basal or insulin-stimulated Akt phosphorylation was similar in cells from normal and GDM pregnancies (Fig. 5*B*). Wortmannin blocked insulin's effect but did not alter basal Akt phosphorylation.

As previously mentioned, insulin did not restored lower V_{max}/K_m values for hENT1-adenosine transport detected in ^{KD}IR-A cells from GDM compared with cells from normal pregnancies (Table 2). However, in the presence of PD-98059 but not wortmannin insulin recovered hENT1-adenosine transport. In ^{KD}IR-B cells from GDM pregnancies, the effect of insulin and inhibitors was similar to nontransduced cells from GDM. Insulin's increase in p42/44^{mapk} phosphorylation was lower in ^{KD}IR-A or ^{KD}IR-B cells from normal pregnancies; however, p42/44^{mapk} phosphorylation was unaltered in these cells in the absence of insulin (Fig. 5*C*). Reduction in the p42/44^{mapk} phosphorylation caused by insulin in GDM pregnancies was blocked in ^{KD}IR-A, but not in ^{KD}IR-B cells. Akt phosphorylation was similarly increased by insulin in cells from normal or GDM pregnancies, an effect blocked in ^{KD}IR-B but not in ^{KD}IR-A cells (Fig. 5*D*).

DISCUSSION

Adenosine transport occurs mainly *via* hENT1 in HUVECs (5, 12, 24, 25). We reported lower hENT1 expression and V_{max}/K_m for adenosine transport in HUVECs from GDM compared with normal pregnancies (5, 25), a phenomenon restored by insulin (5). These results are complemented

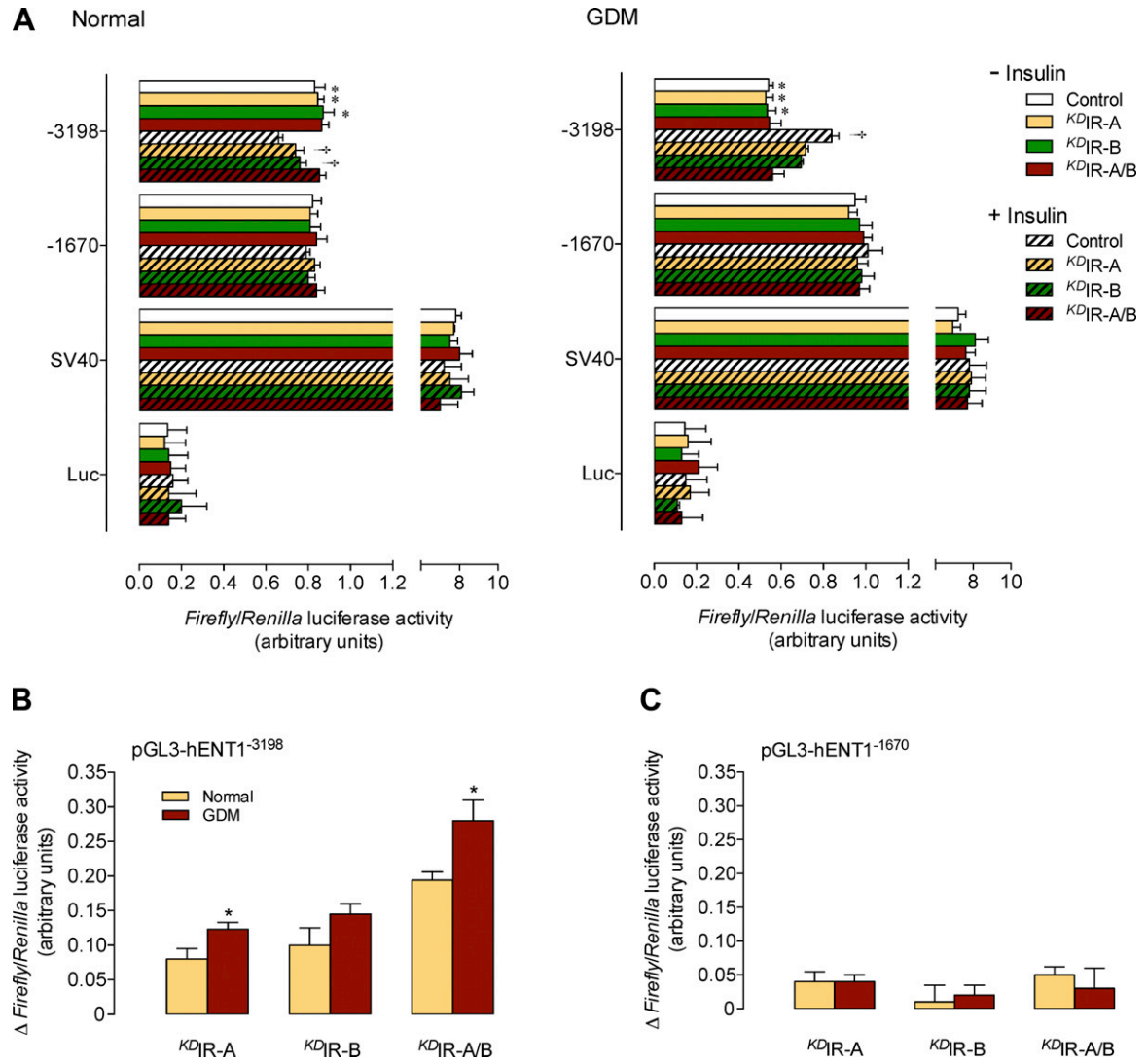

Figure 4. Insulin restores *SLC29A1* promoter activity *via* IR-A in GDM. *A*) Luciferase reporter activity was measured in cells transfected with *SLC29A1* promoter truncations pGL3-hENT1^{-3198} and pGL3-hENT1^{-1670} (see Materials and Methods) that were transduced with adenovirus containing siRNA against IR isoform A (^{KD}IR-A), B (^{KD}IR-B), or both (^{KD}IR-A/B), from normal or GDM pregnancies. Control are nontransduced cells. Assays were in the absence (–Insulin) or presence (+Insulin) of insulin (1 nM, 8 h). *B*) Fraction of change (Δ) in reporter activity caused by insulin in nontransduced *vs.* ^{KD}IR-A, ^{KD}IR-B, or ^{KD}IR-A/B cells transfected with pGL3-hENT1^{-3198}. *C*) As in *B* for cells transfected with pGL3-hENT1^{-1670}. *A*) $^{*}P < 0.05$ and $^{\dagger}P < 0.05$ *vs.* corresponding values for pGL3-hENT1^{-3198} in +Insulin in cells from normal or GDM pregnancies. *B*) $^{*}P < 0.05$ *vs.* corresponding values in cells from normal pregnancies. Values are mean ± SEM ($n = 12$).

by findings showing that hENT1 protein preferentially locates at the plasma membrane in HUVECs from normal pregnancies, but it is mainly intracellular in cells from GDM (confirming previous observations in these cell types) (26), and that these effects are reversed by insulin in fetal endothelial cells from diabetic mothers. HUVECs (5) and hPMECs (6) express at least 2 IRs (*i.e.,* IR-A, preferentially expressed in the placenta and other fetal tissues, and IR-B, preferentially expressed in adult tissues) (19). Insulin reverses diminished hENT2-adenosine transport caused by GDM requiring both IR-A and IR-B expression in hPMECs (6). However, IR-A overexpression could result in lower hENT1 expression and V_{max}/K_m in HUVECs from GDM because the benefit of insulin on hENT1-adenosine transport was absent in ^{KD}IR-A cells. These observations are similar to reports of preferential IR-A expression in skeletal muscle fibers of patients with myotonic dystrophy types 1 (MDT1) and 2 (27, 28) and in ovarian (29), breast (30), colon (31), or thyroid (32) cancer patients. However, because HUVECs from normal or GDM pregnancies were cultured in the presence of 2% sera (final insulin concentration 0.02 nM) compared with 0.04 or 0.07 nM insulin, respectively, in the umbilical vein blood, we cannot rule out the possibility that response to exogenous insulin was due to insulin deprivation *in vitro*. Interestingly, the insulin concentration required to correct alterations of adenosine transport and IRs phosphorylation in HUVECs from GDM was 2.9-fold the circulating insulin in umbilical vein blood in GDM. Thus, even when fetal insulinemia in GDM is higher than in normal pregnancies, this condition is not enough to restore HUVEC function. These data agree with findings in hPMEC from GDM (6) and suggest a potential chronic

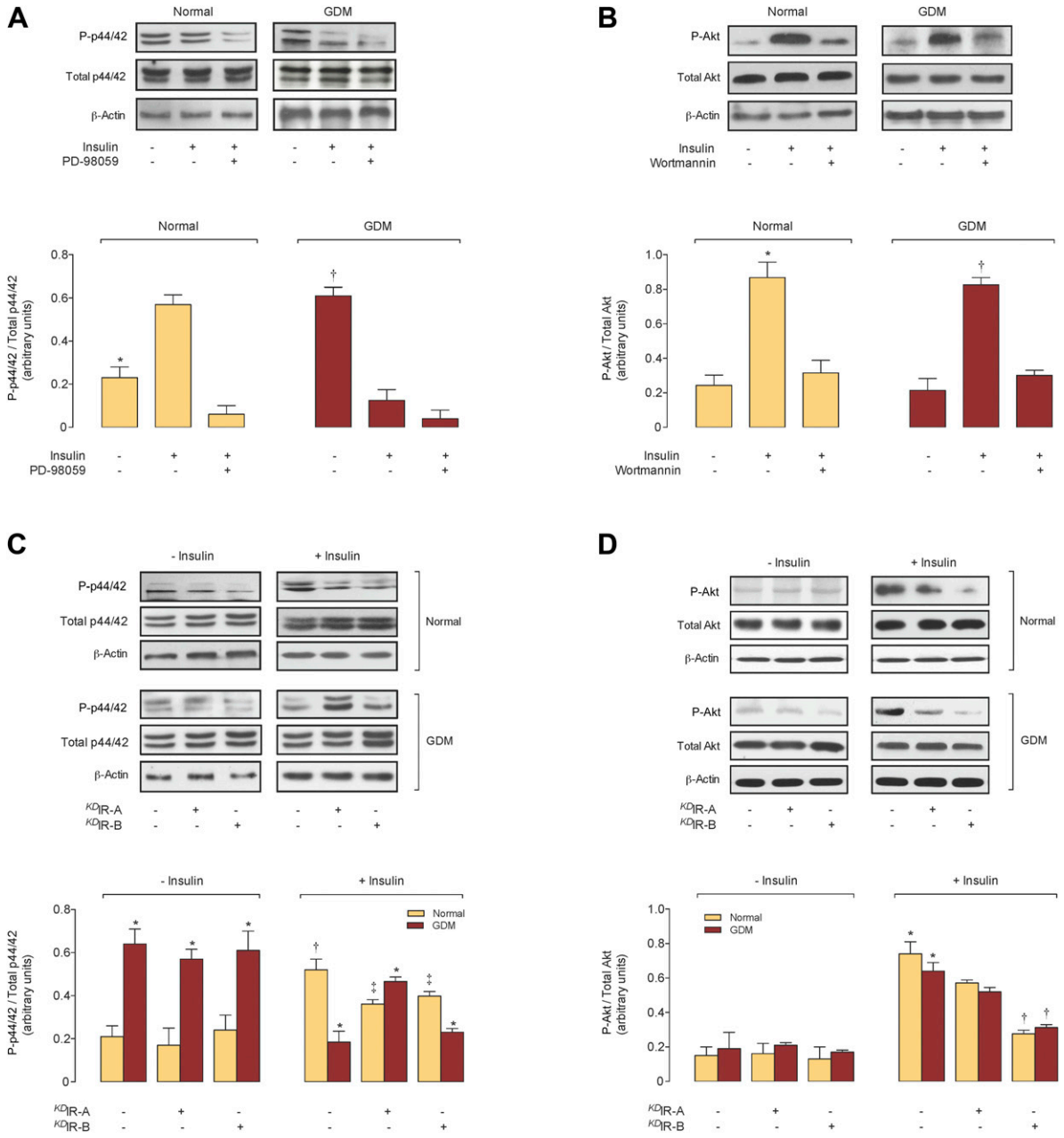

Figure 5. Insulin causes differential activation of p44/42^{mapk} and Akt in GDM and requires IR-A expression to reduce p44/42^{mapk} phosphorylation level in GDM. *A*) Western blot for total (total p44/42) or phosphorylated (P-p44/42) p44/42^{mapk} in HUVEC from normal or GDM pregnancies in the absence (–) or presence (+) of insulin (1 nM, 8 h) or PD-98059 (10 μM, 8 h). β-Actin is internal reference. Lower panel: P-p44/42:total p44/42^{mapk} ratio densitometries. *B*) Western blot for total (total Akt) or phosphorylated (P-Akt) Akt in the absence or presence of insulin or wortmannin (30 nM) as in *A*. Lower panel: P-Akt:total Akt ratio densitometries. *C*) Western blot for total p44/42 or P-p44/42 in nontransduced (–) or transduced (+) cells with adenovirus containing siRNA against IRs isoform A (^{KD}IR-A) or B (^{KD}IR-B), in the absence (–Insulin) or presence (+Insulin) of insulin as in *A*. Lower panel: P-p44/42:total p44/42 ratio densitometries. *D*) Western blot for total Akt or P-Akt as in C. Lower panel: P-Akt: total Akt ratio densitometries. *A*) $^{*}P < 0.04$ and $^{\dagger}P < 0.03$ *vs.* all other corresponding values. *B*) $^{*}P < 0.03$ and $^{\dagger}P < 0.03$ *vs.* all other corresponding values. *C*) $^{*}P < 0.04$ *vs.* corresponding values in normal, $^{\dagger}P < 0.04$ *vs.* all other values in normal, $\ddagger P < 0.05$ *vs.* corresponding values in normal in –Insulin. *D*) $^{*}P < 0.02$ *vs.* all other corresponding values except for ^{KD}IR-A in +Insulin. $^{\dagger}P < 0.05$ *vs.* corresponding values in ^{KD}IR-A in +Insulin. Values are mean ± SEM (n = 12).

insulin resistance of HUVECs from GDM such that they require more insulin to normalize signaling. Because maternal blood adenosine was similar in GDM and normal pregnancies but umbilical cord blood adenosine was higher in GDM compared with normal pregnancies (5, 6), higher adenosine newborn blood at birth is not likely due to an increased transplacental transfer. The latter is supported by findings showing that GDM associates with unaltered maximal [^{3}H]NBTI-specific binding in human syncytiotrophoblast apical membrane vesicles (33). However, we cannot rule out the possibility of an increased adenosine mother-to-fetus transfer in the human placenta in GDM pregnancies to explain increased umbilical vein blood adenosine in GDM (10).

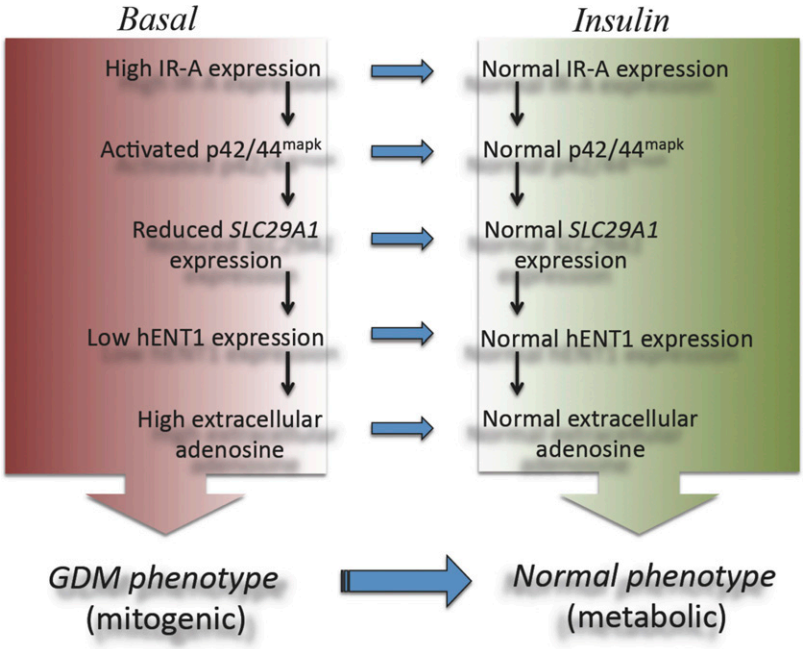

Figure 6. Insulin effect on hENT1-adenosine transport in HUVEC from GDM. Under basal conditions (Basal), HUVEC from GDM exhibit increased expression of IR-A (IR-A) isoform compared with normal pregnancies. This phenomenon leads to increased p42/44^{mapk} resulting in lower *SLC29A1* gene promoter activity and lower expression (mRNA and protein) of hENT1. Thus, lower adenosine uptake and extracellular accumulation of this nucleoside is seen in this cell type. In the presence of insulin, IR-A expression level is restored, a phenomenon resulting in normal p42/44^{mapk} activation and subsequent restoration of *SLC29A1* promoter activity and hENT1 expression and availability at the plasma membrane. As a result of the changes caused by insulin, a restoration of hENT1-mediated adenosine transport leads to physiologic (normal) extracellular levels of adenosine. Thus, HUVEC from GDM exhibiting a mitogenic-like phenotype (GDM phenotype) are reversed to a metabolic-like phenotype (normal phenotype) by insulin.

IR-A and IR-B expression are required for the effect of insulin on adenosine transport in HUVECs from normal pregnancies, thus they equally signal *via* IR-A and IR-B to maintain an equilibrium for a mitogenic/metabolic phenotype (p42/44^{mapk}/Akt activity ~1), as in hPMECs (6). However, because IR-A is overexpressed, a preferential mitogenic (p42/44^{mapk}/Akt activity > 1) instead of a metabolic (p42/44^{mapk}/Akt activity < 1) like phenotype is feasible in HUVECs from GMD. Interestingly, IR-A overexpression is reported in diseases featuring severe insulin resistance, including MDT1 (27, 28). HOMA-IR in human newborns from GDM pregnancies (HOMA-IR ~2.8) (6, 34) is similar to our data. GDM-increased HOMA-IR could cause abnormal hENT1-adenosine transport due to lower insulin sensitivity in HUVECs from GDM and this is in agreement with reported positive correlations for maternal and fetal insulin resistance in GDM (6, 34). However, we cannot rule out the possibility that GDM-associated alterations may result from a potential prebirth insulin resistant state. Although total β-IR protein abundance in GDM was lower compared with normal pregnancies, IRs activation appears to be unaltered by GDM because insulin-increased β-IR phosphorylation (*i.e.,* activation) was similar in both cell types. However, because SC_{50} for insulin as an activator of β-IR in ^{KD}IR-A cells from normal pregnancies was ~1.8-fold that in ^{KD}IR-A cells from GDM pregnancies and because insulin reversed IR-A expression in cells from GDM to more normal values in the absence of insulin, normal IR-A expression is required for a proper insulin-increased β-IR phosphorylation in HUVECs. Because HOMA-IR values for newborns from GDM was ~2.4-fold greater than normal pregnancies, newborn insulin resistance could result from higher IR-A expression. IR-A and IR-B differential involvement for insulin response is not a generalized finding for fetal macrovascular endothelium because insulin modulation of hENT2-adenosine transport requires IR-A and IR-B expression in hPMECs from GDM (6).

Reduction of hENT1-adenosine transport coincided with lower *SLC29A1* and *hENT1* mRNA expression but with IR-A overexpression in GDM. These receptors may play a role in the deleterious effects of GDM in HUVECs; some of insulin's effect requiring IR-A expression to reverse GDM-reduced *SLC29A1* promoter transcriptional activity, and *hENT1* mRNA expression and protein abundance were higher in GDM *vs.* normal pregnancies. Expression of both IR forms was required for *hENT1* mRNA expression but not for protein abundance or *SLC29A1* promoter activity in GDM HUVECs. Possibly, changes in mRNA stability were modulated by both IRs (not just IR-A) in this cell type.

Insulin reversed the GDM-associated increase in p42/44^{mapk} phosphorylation, an effect abolished only in ^{KD}IR-A cells, suggesting that insulin requires a minimum level of IR-A expression to activate p42/44^{mapk} signaling in HUVECs. This finding agrees with preferential increases in p42/44^{mapk} phosphorylation by insulin activation of IR-A in a HeLa cell line (35). However, the PI3K/Akt pathway is unaltered by GDM in HUVECs; insulin-increased Akt phosphorylation was similar in normal and GDM pregnancies. In addition, insulin-stimulated PI3K/Akt signaling was abolished in ^{KD}IR-B cells in normal and GDM pregnancies, suggesting that insulin requires a minimum level of IR-B expression to activate PI3K/Akt signaling, as in other cell types (35). In contrast, basal p42/44^{mapk} and Akt phosphorylation is independent of IR-A or IR-B expression in normal and GDM pregnancies. HUVECs from normal pregnancies may require expression of both IRs for insulin activation of these cell signaling molecules. Thus, an equilibrated mitogenic:metabolic ratio phenotype of HUVECs from normal pregnancies compared with a preferential mitogenic phenotype in GDM is suggested (5).

GDM activates p42/44^{mapk} leading to hENT1-reduced transport, but insulin reversal of this change does not involve these molecules in HUVECs. Alternatively, insulin increased p42/44^{mapk}, and Akt phosphorylation in GDM could be due to a crosstalk of these signaling pathways, a phenomenon that could also be the case in normal pregnancies because insulin-reduced hENT1-adenosine transport was blocked by PD-98059 or wortmannin. When

IR-A expression was restored in HUVECs from GDM, insulin's effect on transport was abolished but because only PD-98059 restored insulin's effect in this cell type; a basal, non-IR-A-dependent p42/44^{mapk} activation, mimicking the GDM phenotype with normal IR-A expression, persisted. This was restricted to GDM because insulin's effect on transport in ^{KD}IR-A from normal pregnancies was reversed by PD-98059 or wortmannin, thus involving both p42/44^{mapk} and PI3K/Akt pathways in this cell type. Because insulin effect was still present in ^{KD}IR-B cells or in the presence of wortmannin, insulin response did not involve PI3K/Akt in GDM. The latter is paralleled by results showing that hENT1-adenosine transport was unaltered in ^{KD}IR-B or by wortmannin. On the contrary, in ^{KD}IR-B cells from normal pregnancies, p42/44^{mapk} and PI3K/Akt pathway involvement is likely.

In summary, we report that HUVECs from GDM pregnancies are functionally altered due to differential IR expression. HUVECs from GDM have a predominantly mitogenic phenotype due to IR-A overexpression, compared with a predominant metabolic phenotype in normal pregnancies. Insulin reverses these alterations *via* lower p42/44^{mapk} but not Akt cell signaling (**Fig. 6**). Insulin restores *SLC29A1* expression and hENT1 transport activity. We propose that insulin's effect on hENT1-adenosine transport is due to normalization of IR-A expression in HUVECs from GDM, requiring a normal, but not totally abolished, expression of this IR form to secure insulin activation of HUVEC metabolism. This phenomenon could be of clinical relevance for vascular hemodynamics of the fetoplacental circulation under conditions of insulin resistance such as GDM (5, 6, 34). Insulin's response by the placental vasculature may differ depending on the IR isoform preferentially activated. Because umbilical veins from GDM pregnancies have a tonic dilation higher than in normal pregnancies, perhaps due to increased circulating adenosine (5), and even when systemic fetal adenosine is unknown (10), these results may help strategize treatment of patients' course with GDM pregnancies, securing the well-being of the growing fetus in this disease. FJ

The authors thank Mrs. Amparo Pacheco and Mrs. Ninoska Muñoz from the Cellular and Molecular Physiology Laboratory (CMPL) at Division of Obstetrics and Gynaecology, Faculty of Medicine, Pontificia Universidad Católica de Chile, for excellent technical and secretarial assistance, respectively, and the personnel of the Hospital Clínico Pontificia Universidad Católica de Chile labor ward for the supply of placentas. This study was supported by Fondo Nacional de Desarrollo Científico y Tecnológico (FONDECYT 1110977, 11110059, 3140516, 3130583, 3140532), Santiago, Chile; Programa de Investigación Interdisciplinario (PIA) from Comisión Nacional de Investigación en Ciencia y Tecnología (CONICYT Anillos ACT-73); and International NETWORK program (CONICYT 130102). T.S. holds a CONICYT-Ph.D. (Santiago, Chile) fellowship. R.S. is recipient of a Faculty of Medicine, Pontificia Universidad Católica de Chile-Ph.D. fellowship. The authors declare no conflicts of interest.

REFERENCES

1. American Diabetes Association. (2014) Diagnosis and classification of diabetes mellitus. *Diabetes Care* **37**(Suppl 1), S81–S90
2. Metzger, B. E., Buchanan, T. A., Coustan, D. R., de Leiva, A., Dunger, D. B., Hadden, D. R., Hod, M., Kitzmiller, J. L., Kjos, S. L., Oats, J. N., Pettitt, D. J., Sacks, D. A., and Zoupas C. (2007) Summary and recommendations of the Fifth International Workshop-Conference on Gestational Diabetes Mellitus. *Diabetes Care* **30**(Suppl 2), S251–S260; Erratum in *Diabetes Care.* 2007 Dec; 30(12):3154
3. Colomiere, M., Permezel, M., Riley, C., Desoye, G., and Lappas, M. (2009) Defective insulin signaling in placenta from pregnancies complicated by gestational diabetes mellitus. *Eur. J. Endocrinol.* **160**, 567–578
4. Hiden, U., Lang, I., Ghaffari-Tabrizi, N., Gauster, M., Lang, U., and Desoye, G. (2009) Insulin action on the human placental endothelium in normal and diabetic pregnancy. *Curr. Vasc. Pharmacol.* **7**, 460–466
5. Westermeier, F., Salomón, C., González, M., Puebla, C., Guzmán-Gutiérrez, E., Cifuentes, F., Leiva, A., Casanello, P., and Sobrevia, L. (2011) Insulin restores gestational diabetes mellitus-reduced adenosine transport involving differential expression of insulin receptor isoforms in human umbilical vein endothelium. *Diabetes* **60**, 1677–1687
6. Salomón, C., Westermeier, F., Puebla, C., Arroyo, P., Guzmán-Gutiérrez, E., Pardo, F., Leiva, A., Casanello, P., and Sobrevia, L. (2012) Gestational diabetes reduces adenosine transport in human placental microvascular endothelium, an effect reversed by insulin. *PLoS ONE* **7**, e40578
7. Maguire, M. H., Szabó, I., Valkó, I. E., Finley, B. E., and Bennett, T. L. (1998) Simultaneous measurement of adenosine and hypoxanthine in human umbilical cord plasma using reversed-phase high-performance liquid chromatography with photodiode-array detection and on-line validation of peak purity. *J. Chromatogr. B Biomed. Sci. Appl.* **707**, 33–41
8. Guzmán-Gutiérrez, E., Westermeier, F., Salomón, C., González, M., Pardo, F., Leiva, A., and Sobrevia, L. (2012) Insulin-increased L-arginine transport requires A(2A) adenosine receptors activation in human umbilical vein endothelium. *PLoS ONE* **7**, e41705
9. Sobrevia, L., Abarzúa, F., Nien, J. K., Salomón, C., Westermeier, F., Puebla, C., Cifuentes, F., Guzmán-Gutiérrez, E., Leiva, A., and Casanello, P. (2011) Review: Differential placental macrovascular and microvascular endothelial dysfunction in gestational diabetes. *Placenta* **32**(Suppl 2), S159–S164
10. Guzmán-Gutiérrez, E., Arroyo, P., Salsoso, R., Fuenzalida, B., Sáez, T., Leiva, A., Pardo, F., and Sobrevia, L. (2014) Role of insulin and adenosine in the human placenta microvascular and macrovascular endothelial cell dysfunction in gestational diabetes mellitus. *Microcirculation* **21**, 26–37
11. Burnstock, G., and Novak, I. (2013) Purinergic signalling and diabetes. *Purinergic Signal.* **9**, 307–324
12. Farías, M., Puebla, C., Westermeier, F., Jo, M. J., Pastor-Anglada, M., Casanello, P., and Sobrevia, L. (2010) Nitric oxide reduces SLC29A1 promoter activity and adenosine transport involving transcription factor complex hCHOP-C/EBPalpha in human umbilical vein endothelial cells from gestational diabetes. *Cardiovasc. Res.* **86**, 45–54
13. Young, J. D., Yao, S. Y., Baldwin, J. M., Cass, C. E., and Baldwin, S. A. (2013) The human concentrative and equilibrative nucleoside transporter families, SLC28 and SLC29. *Mol. Aspects Med.* **34**, 529–547
14. Vásquez, G., Sanhueza, F., Vásquez, R., González, M., San Martín, R., Casanello, P., and Sobrevia, L. (2004) Role of adenosine transport in gestational diabetes-induced L-arginine transport and nitric oxide synthesis in human umbilical vein endothelium. *J. Physiol.* **560**, 111–122
15. San Martín, R., and Sobrevia, L. (2006) Gestational diabetes and the adenosine/L-arginine/nitric oxide (ALANO) pathway in human umbilical vein endothelium. *Placenta* **27**, 1–10
16. Belfiore, A., Frasca, F., Pandini, G., Sciacca, L., and Vigneri, R. (2009) Insulin receptor isoforms and insulin receptor/insulin-like growth factor receptor hybrids in physiology and disease. *Endocr. Rev.* **30**, 586–623
17. Ullrich, A., Bell, J. R., Chen, E. Y., Herrera, R., Petruzzelli, L. M., Dull, T. J., Gray, A., Coussens, L., Liao, Y. C., Tsubokawa, M., Mason, A., Seeburg, P. H., Grunfeld, C., Rosen, O. M., and Ramachandran, J. (1985) Human insulin receptor and its relationship to the tyrosine kinase family of oncogenes. *Nature* **313**, 756–761
18. Ebina, Y., Edery, M., Ellis, L., Standring, D., Beaudoin, J., Roth, R. A., and Rutter, W. J. (1985) Expression of a functional human insulin receptor from a cloned cDNA in Chinese hamster ovary cells. *Proc. Natl. Acad. Sci. USA* **82**, 8014–8018

19. Frasca, F., Pandini, G., Sciacca, L., Pezzino, V., Squatrito, S., Belfiore, A., and Vigneri, R. (2008) The role of insulin receptors and IGF-I receptors in cancer and other diseases. *Arch. Physiol. Biochem.* **114**, 23–37
20. Matthews, D. R., Hosker, J. P., Rudenski, A. S., Naylor, B. A., Treacher, D. F., and Turner, R. C. (1985) Homeostasis model assessment: insulin resistance and beta-cell function from fasting plasma glucose and insulin concentrations in man. *Diabetologia* **28**, 412–419
21. Wang, Y. H., Wu, H. H., Ding, H., Li, Y., Wang, Z. H., Li, F., and Zhang, J. P. (2013) Changes of insulin resistance and β-cell function in women with gestational diabetes mellitus and normal pregnant women during mid- and late pregnant period: a case-control study. *J. Obstet. Gynaecol. Res.* **39**, 647–652
22. Antonov, J., Goldstein, D. R., Oberli, A., Baltzer, A., Pirotta, M., Fleischmann, A., Altermatt, H. J., and Jaggi, R. (2005) Reliable gene expression measurements from degraded RNA by quantitative real-time PCR depend on short amplicons and a proper normalization. *Lab. Invest.* **85**, 1040–1050
23. Li, G., Barrett, E. J., Wang, H., Chai, W., and Liu, Z. (2005) Insulin at physiological concentrations selectively activates insulin but not insulin-like growth factor I (IGF-I) or insulin/IGF-I hybrid receptors in endothelial cells. *Endocrinology* **146**, 4690–4696
24. Molina-Arcas, M., Casado, F. J., and Pastor-Anglada, M. (2009) Nucleoside transporter proteins. *Curr. Vasc. Pharmacol.* **7**, 426–434
25. Farías, M., San Martín, R., Puebla, C., Pearson, J. D., Casado, J. F., Pastor-Anglada, M., Casanello, P., and Sobrevia, L. (2006) Nitric oxide reduces adenosine transporter ENT1 gene (*SLC29A1*) promoter activity in human fetal endothelium from gestational diabetes. *J. Cell. Physiol.* **208**, 451–460
26. Sobrevia, L., Puebla, C., Farías, M., and Casanello, P. (2009) Role of equilibrative nucleoside transporters in fetal endothelial dysfunction in gestational diabetes. In *Membrane Transporters and Receptors in Disease* (Sobrevia, L., and Casanello, P., eds.), pp. 1–25, Research Signpost, Kerala, India
27. Savkur, R. S., Philips, A. V., and Cooper, T. A. (2001) Aberrant regulation of insulin receptor alternative splicing is associated with insulin resistance in myotonic dystrophy. *Nat. Genet.* **29**, 40–47
28. Santoro, M., Masciullo, M., Bonvissuto, D., Bianchi, M. L., Michetti, F., and Silvestri, G. (2013) Alternative splicing of human insulin receptor gene (INSR) in type I and type II skeletal muscle fibers of patients with myotonic dystrophy type 1 and type 2. *Mol. Cell. Biochem.* **380**, 259–265
29. Phy, J. L., Conover, C. A., Abbott, D. H., Zschunke, M. A., Walker, D. L., Session, D. R., Tummon, I. S., Thornhill, A. R., Lesnick, T. G., and Dumesic, D. A. (2004) Insulin and messenger ribonucleic acid expression of insulin receptor isoforms in ovarian follicles from nonhirsute ovulatory women and polycystic ovary syndrome patients. *J. Clin. Endocrinol. Metab.* **89**, 3561–3566
30. Kalla Singh, S., Brito, C., Tan, Q. W., De León, M., and De León, D. (2011) Differential expression and signaling activation of insulin receptor isoforms A and B: A link between breast cancer and diabetes. *Growth Factors* **29**, 278–289
31. Brierley, G. V., Macaulay, S. L., Forbes, B. E., Wallace, J. C., Cosgrove, L. J., and Macaulay, V. M. (2010) Silencing of the insulin receptor isoform A favors formation of type 1 insulin-like growth factor receptor (IGF-IR) homodimers and enhances ligand-induced IGF-IR activation and viability of human colon carcinoma cells. *Endocrinology* **151**, 1418–1427
32. Malaguarnera, R., Frasca, F., Garozzo, A., Gianì, F., Pandini, G., Vella, V., Vigneri, R., and Belfiore, A. (2011) Insulin receptor isoforms and insulin-like growth factor receptor in human follicular cell precursors from papillary thyroid cancer and normal thyroid. *J. Clin. Endocrinol. Metab.* **96**, 766–774
33. Osses, N., Sobrevia, L., Cordova, C., Jarvis, S. M., and Yudilevich, D. L. (1995) Transport and metabolism of adenosine in diabetic human placenta. *Reprod. Fertil. Dev.* **7**, 1499–1503
34. Wang, Q., Huang, R., Yu, B., Cao, F., Wang, H., Zhang, M., Wang, X., Zhang, B., Zhou, H., and Zhu, Z. (2013) Higher fetal insulin resistance in Chinese pregnant women with gestational diabetes mellitus and correlation with maternal insulin resistance. *PLoS ONE* **8**, e59845
35. Malaguarnera, R., Sacco, A., Voci, C., Pandini, G., Vigneri, R., and Belfiore, A. (2012) Proinsulin binds with high affinity the insulin receptor isoform A and predominantly activates the mitogenic pathway. *Endocrinology* **153**, 2152–2163

Received for publication April 10, 2014.
Accepted for publication September 4, 2014.